Progress in Reaction Kinetics and Mechanism

ARTICLE

Open Access

https://doi.org/10.48130/prkm-0025-0018

Progress in Reaction Kinetics and Mechanism **2025**, 50: e019

Molecular dynamics simulation of pyrolysis in polyethylene cable sheaths under electric field

Shuangshuang Tian[1], Dunpeng Yang[1], Yingyu Wu[1], Chenying Li[2], Benli Liu[1], Nnditshedzeni Eric Maluta[3] and Zhou Huang[1*]

[1] *Hubei Engineering Research Center for Safety Monitoring of New Energy and Power Grid Equipment, Hubei University of Technology, Wuhan 430068, China*
[2] *Electric Power Science Research Institute, State Grid Jiangsu Electric Power Co., Ltd., Nanjing 210000, China*
[3] *Department of Physics, University of Venda, Thohoyandou 0950, South Africa*
* Corresponding author, E-mail: 20171036@hbut.edu.cn

Abstract

Power cable pyrolysis is typically a precursor to combustion. The pyrolytic reaction of the cable during operation is influenced by the electric field. Investigating the mechanisms underlying cable pyrolysis in the presence of an electric field is crucial for preventing cable fires. This paper examines the pyrolysis process and key reaction processes of the polyethylene (PE) sheath of a typical power cable, utilizing the ReaxFF-MD method as a theoretical framework. The effect of temperature on pyrolysis products is studied. The influence of the electric field on pyrolysis products, pathways, and major radical reactions is investigated. The combined effect of the electric field and temperature on PE pyrolysis is also investigated. The results show that the main pyrolysis products of PE are C_2H_4, H_2, C_2H_2, and CH_4, consistent with the conclusions of the pyrolysis product experiments. The total number of pyrolysis products increased in a significant manner with increasing temperature. Under the action of the electric field, the type and number of final products are almost constant. However, the electric field reduces the activation energy of PE pyrolysis. The electric field affects the pyrolysis process by affecting the key reactions of PE pyrolysis. In the initial stages of pyrolysis, PE generates the primary intermediate product C_2H_4, in addition to a minor quantity of H and CH_3 radicals through chain reactions. C_2H_4 is decomposed to form C_2H_2 and dehydrogenates with H to produce H_2. The CH_3 radical combines with the H radical to generate CH_4. The applied electric field made the pyrolysis particles more susceptible to cracking, leading to an increase in the number of CH_4. The electric field has a significant effect on the PE pyrolysis process by regulating the collision frequency of partially reactive molecules. This study reveals the mechanism of the electric field effect on cable pyrolysis and provides an important reference for preventing similar cable fires. It provides an important reference for preventing similar cable fires.

Citation: Tian S, Yang D, Wu Y, Li C, Liu B, et al. 2025. Molecular dynamics simulation of pyrolysis in polyethylene cable sheaths under electric field. *Progress in Reaction Kinetics and Mechanism* 50: e019 https://doi.org/10.48130/prkm-0025-0018

Introduction

Power cables are extensively utilized in industry, primarily for power transmission and transportation. However, during electrical energy transport, cables are prone to various faults such as short-circuiting, overloading, and poor contact. These issues can lead to the burning of cables and potentially cause cable fires. From the moment a cable fails to the onset of burning, the cable sheath undergoes pyrolysis due to rising temperatures. During this pyrolysis process, the sheath thermally decomposes, producing combustible gases that further facilitate cable combustion[1]. Fires can be pre-warned by detecting pyrolysis decomposition products, which are characteristic signals of cable operation and fire[2–6]. Therefore, studying the pyrolysis characteristics of cable sheathing under an electric field is crucial for understanding and preventing cable fires.

Thermogravimetry (TG) is an experimental technique used to study the pyrolysis properties of cables, effectively representing the mass loss during the thermal decomposition of a sample. Based on TG data, researchers employ model-free methods such as the Ozawa method, the KAS method, and the Starink method to calculate the apparent activation energy of the cable sheath[7–10]. This apparent activation energy indicates the thermal stability of the sheath. However, analyzing the pyrolysis products solely through the mass change of the cable sheath during pyrolysis is insufficient. Existing studies suggest that gas chromatography-mass spectrometry (GC-MS) provides a more accurate analysis of pyrolysis products. For example, Chen et al. investigated the main volatile products of iste cable hoses using TG-MS and identified the order of the maximum amounts of four volatile products[11]. Similarly, Qin et al. analyzed the thermal degradation of polystyrene and polypropylene using coupled TG-GC and TG-GC/MS, finding that the initial pyrolysis products mainly included styrene, benzene, toluene, and small amounts of C1–C4 aliphatic hydrocarbons[12]. Most existing studies on cable sheath pyrolysis focus on the macroscopic characteristics of the process. However, there is a lack of detailed research on the specific pyrolysis processes of sheath materials, the primary radical reactions, and the effects of an electric field on pyrolysis characteristics. Therefore, it is crucial to investigate the chemical mechanisms of cable sheath pyrolysis, the principal reaction pathways, and the influence of the electric field on these processes.

Molecular dynamics (MD) simulation is a numerical method used to solve the equations of motion for molecular systems, allowing for the investigation of their structure and properties. However, traditional MD cannot describe the bond-breaking and formation processes involved in chemical reactions[13]. The reactive force field (ReaxFF) developed by van Duin et al. addresses this limitation[14]. ReaxFF's force field parameters are derived from extensive geometric and energetic data, enabling it to characterize complex chemical reactions across various systems[15]. Numerous studies have demonstrated the accuracy of ReaxFF-MD in fields such as catalysis[16–18], coal chemistry[19–21], and nitrogen chemistry[22–24]. Some scholars employ the ReaxFF approach to investigate the pyrolysis characteristics and reaction mechanisms of organic matter. For instance, Pu et al. used ReaxFF-MD calculations to study the pyrolysis mechanisms

of pure HFO-1234yf and R32. Their results showed that R32 inhibits the decomposition of HFO-1234yf at 2,600–2,800 K but promotes its decomposition at temperatures above 3,000 K[25]. Kong et al. studied the distribution of pyrolysis gas-phase products of cross-linked polyethylene cables with ReaxFF, identifying H_2, CH_4, C_2H_6, C_2H_4, and C_2H_2 as the primary gas-phase products[26]. Chao et al. used GC-MS and ReaxFF-MD to investigate polypropylene cables, finding that the main hydrocarbon products in the decomposition are CH_4, C_2H_4, C_3H_6, and C_2H_6[27]. Döntgen et al. successfully deduced the reaction mechanism of high-temperature methane combustion by utilizing ChemTraYzer, and further extending ChemTraYzer to facilitate chemical kinetics studies[28,29]. Sarah et al. analyzed the consumption of cyclohexanone using ChemTrayzer to obtain the product distribution as well as the decomposition pathways[30].

The investigation of the effect of electric fields on pyrolysis has been undertaken by scholars using ReaxFF-MD. Zhou et al. investigated the inhibition mechanism of polycyclic aromatic hydrocarbon (PAH) formation during n-decane pyrolysis using ReaxFF-MD, finding that the electric field accelerates the cleavage reaction rate of n-decane and reduces the enthalpy change of bond cleavage[31]. Zhou et al. examined the influence of electric fields on the pyrolysis reaction paths of JP-10 fuel using ReaxFF-MD. It elucidates that the pyrolysis reaction activation energy and molecular motion are the key factors affected by the co-effect of temperature and electric field[32]. This provides ideas for studying the effect of the electric field on the pyrolysis of cable sheaths.

In this paper, the effect of electric field on the pyrolysis of PE, a typical cable sheath, is investigated by the ReaxFF-MD method. First, the pyrolysis products of polyethylene are investigated and verified by experimental data. Then, the effect of temperature on the generation of polyethylene pyrolysis products is explored. Furthermore, the effects of the electric field on the pyrolysis process involve the effects on pyrolysis products, reaction pathways, and major radical reactions. These findings can offer valuable insights for understanding fire characteristics and preventing similar incidents.

Simulation methodology

Based on Materials Studio, to build a long chain of PE with a degree of polymerization of 50. PE cells containing ten long chains are built by the Amorphous Cell module. The density of the system is set to 0.92 g/cm^3. The PE model is subjected to five annealing cycles of 300–500 K by the COMPASS II (Condensed-phase molecular potentials for atomistic simulation studies II) force field. The system is subsequently kinetically equilibrated by the NVT system at room temperature and atmospheric pressure for 100 ps with the step size set to 0.5 fs. In order to better reflect the molecular dynamics processes of gas molecules in the PE system, the Berendsen method is used as a thermostat. Then electrostatic and van der Waals forces are respectively treated by the Ewald method and the Atom-based method. Finally, the optimized PE pyrolysis model is obtained as shown in Fig. 1.

The PE model optimized by Materials Studio is imported into ReaxFF and subjected to a relaxation process at 5 K to avoid bond link among molecules and equilibrate the system energy. During the relaxation phase, the force field is selected to be CHOSFCIN.ff, with a total time of 50 ps and a step size of 0.25 fs[33]. To gain deeper insight into how different temperatures and electric fields influence the pyrolysis of polyethylene cable sheaths, the electric field strength is set, taking into account the actual use of PE sheaths and with reference to the electric field gradient setting method of Zhou et al.[31]. Molecular dynamics simulations are performed at specific temperature points (2,500, 2,700, 2,900, 3,100, and 3,300 K), and at

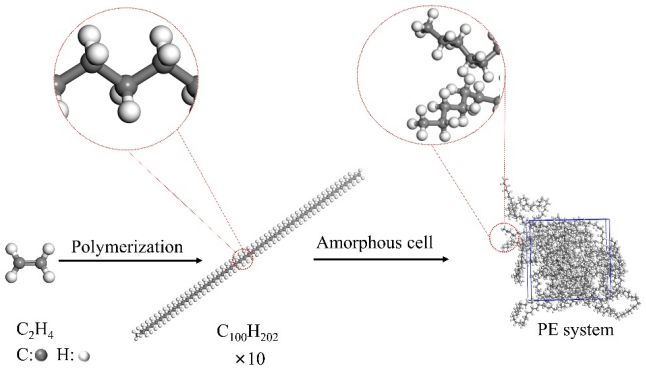

Fig. 1 PE pyrolysis model.

different electric field strengths (0, 0.003, and 0.03 V/Å). It is not difficult to find that the simulated temperature is much higher than the experimental temperature, which is due to the fact that the time scale of the simulation is only in the ps level, which is much lower than that of the experimental conditions. This has been investigated in the literature, and it is found that the reaction mechanism and kinetic results obtained by high-temperature simulation are more consistent with those obtained experimentally[34,35]. Each molecular dynamics simulation is executed for 2,000 ps with a time step of 0.1 fs, and the resulting data are averaged over three simulations of the molecular system with disparate initial states. All the above processes are simulated in molecular dynamics under an NVT system with atmospheric pressure, and NHC is used as a thermostat. The formation and breakage of chemical bonds are analyzed by the Chemtrayzer module, which in turn investigates the pyrolysis pathways and the mechanism of electric field influence on PE pyrolysis.

Results and discussion

Main pyrolysis products

In this paper, the major pyrolysis particles are found to be C_2H_4, C_2H_2, H_2, C_2H_3, CH_3, CH_4, C_3H_6, C_3H_5, C_3H_4, C_3H_3, and H. Among them, C_3H_6, C_3H_5, C_3H_4, C_2H_4, and C_2H_2 are characterized by different structures as shown in Fig. 2. As can be seen in Fig. 2, only C_3H_4 exhibits isomerization in all these species, which account for a relatively small percentage of the major pyrolysis products, and ultimately C_2H_2 is produced by thermal decomposition.

The change rule of the main pyrolysis species C_2H_4, C_2H_2, H_2, C_2H_3, CH_3, CH_4, C_3H_6, C_3H_5, C_3H_4, C_3H_3, and H under the condition of the temperature of 3,100 K is obtained as shown in Fig. 3. The number of the intermediate product C_2H_4 increases rapidly within the first 60 ps of the pyrolysis reaction. This is due to the homolytic cleavage of the C-C and C-H bonds in the long-chain molecules of polyethylene, resulting in the production of a large number of alkyl radicals. Long-chain alkyl radicals tend to break at the second carbon (β-carbon)

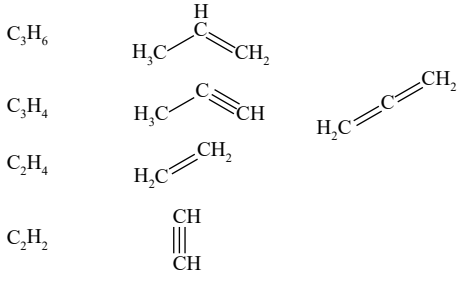

Fig. 2 Isomers of major pyrolysis products.

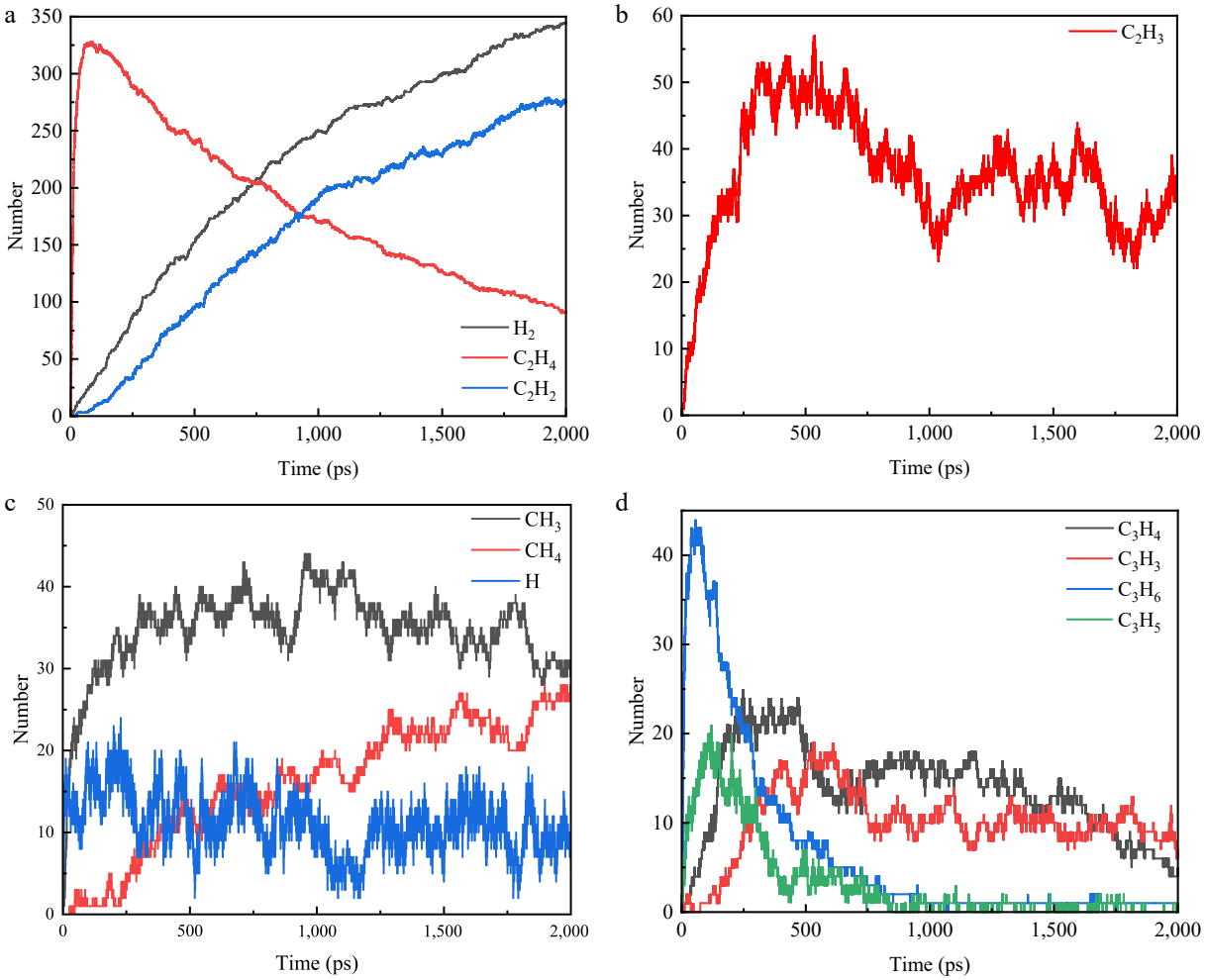

Fig. 3 Variation curve of the number of main pyrolysis particles (total number of isomers) with time. (a) C_2H_2, C_2H_4, H_2. (b) C_2H_3. (c) CH_3, CH_4, H. (d) C_3H_6, C_3H_5, C_3H_4, C_3H_3.

from the radical position. The break produces a C_2H_4 and a new, shorter alkyl radical. Also, hydrogen transfer within the molecule increases the number of C_2H_4. After 60 ps, the number of C_2H_4 shows a significant decrease. C_2H_4 is unstable at high temperatures and can be further dehydrogenated to form C_2H_2 and H_2. The β-break or hydrogen-robbing reaction may also first produce C_2H_3, a very reactive radical that can easily lose an H radical to form C_2H_2. Although acetylene has a high bond energy, its enthalpy of formation is very high, and its high entropy value at high temperatures makes it a dominant product. When two radicals meet and combine, sometimes instead of forming a C-C bond, the two hydrogen atoms combine to form H_2, leaving an unsaturated bond (usually a double bond). At higher temperatures, the radical site may seize the hydrogen of neighboring carbons on its own chain, generating a direct double bond and H_2 (or H radicals, but H radicals are highly susceptible to bonding to H_2). Although not as prevalent as β-fracture, it also contributes to H_2 under certain conditions. This stabilizes the number of C_2H_2 and H_2 rising cleavage occurrences near the terminal methyl group of the polymer chain. The resulting CH_3 can undergo a hydrogen capture reaction to form CH_4. Observation indicates that the C3 (C_3H_6, C_3H_5, C_3H_4, and C_3H_3) products exhibit a tendency to increase and then decrease. Furthermore, the higher the H content, the more these products disappear completely first. This suggests that the C3 and above particles are unable to exist under these conditions and decompose into products with a smaller number of carbons. The final products are therefore H_2, C_2H_2, C_2H_4, and a small amount of CH_4.

To verify the accuracy of the theoretical calculations, the PE sheath material of a high-voltage cable (YJLW03Z-64/110 KV) is selected for pyrolysis experiments, and the gas products are examined using oil chromatography. Literature is reviewed to determine the major product of PE sheath decomposition, and a standard gas is selected to calibrate the oil chromatogram based on this major product. Since the background gas for the pyrolysis experiment is nitrogen, nitrogen is selected as the background gas for the assay. After completing the calibration, 1 mL of pyrolysis gas is injected for testing and subsequently analyzed for the type of gas and its content. The experimental temperature, experimental atmosphere, airflow purging rate, and temperature increasing rate are set to 30–800 °C, nitrogen, 50 mL/min, and 10 °C/min, which are respectively. As shown in Fig. 4, the detected gas products mainly consist of CH_4, C_2H_4, H_2, and C_2H_2, and it is obvious that the experimental products are consistent with the simulation products.

Effect of temperature on pyrolysis

To study the effect of different temperatures on the pyrolysis of the cable sheath, the changes in the number of major products at five temperatures, 2,500, 2,700, 2,900, 3,100, and 3,300 K, are calculated (Fig. 5). The result indicates that the total number of pyrolysis products increases significantly with the temperature. As illustrated in Fig. 5a–c, the alterations in C_2H_4, C_2H_2, and H_2 are minimal at

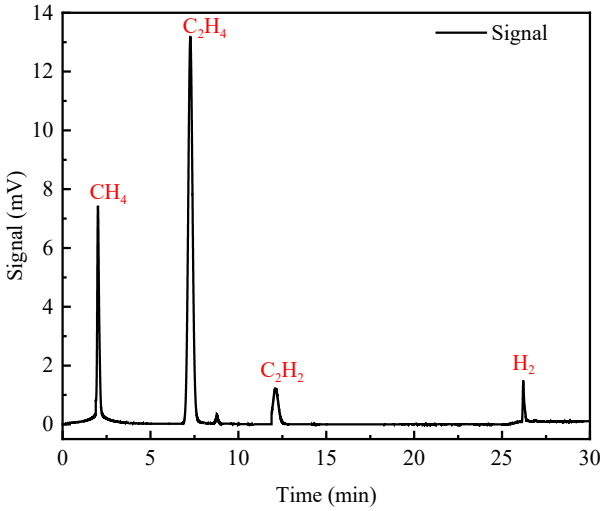

Fig. 4 PE pyrolysis components.

2,500 and 2,700 K, suggesting that temperature exerts a negligible influence on the pyrolysis products at low temperatures. Figure 5d shows that CH_4 varies less between 2,700 and 3,300 K. In comparison, the number is significantly lower at 2,500 K, indicating that less CH_4 is generated at low temperatures, and its number increases significantly and stabilizes beyond a certain temperature. As shown in Fig. 5e, the trend of the number of C_3H_6 is approximately the same as that of C_2H_4. This indicates that C_3H_6 is also an intermediate product, but it is completely decomposed as the temperature increases. Figure 5f reveals a significant increase in the concentration of H atoms with increasing temperature, suggesting a further increase in the vigor of the reaction. This indicates that the breakage of PE long chains is accelerated at high temperatures, generating a large number of substituents (e.g., C_2H_3 and C_2H_5) as well as H atoms, which leads to an increase in the total number of molecules in the system.

Effect of electric fields on pyrolysis

To investigate the effect of electric field on the kinetic properties of PE pyrolysis, a first-order kinetic approach is used[36].

The concentration of PE is represented by its molecular number, and k is obtained from a linear fit of Nt and t, that is:

$$\ln(\mathrm{N}t) - \ln(\mathrm{N0}) = -\mathrm{k}t \quad (1)$$

where, N0 denotes the initial number of reactants, k is the reaction rate constant, t denotes the reaction time, and Nt denotes the number of reactants at time t.

Fitting Eq. (1) yielded the rate constants of three types of electric field (0, 0.003, and 0.03 V/Å) at different pyrolysis temperatures, as shown in Table 1. The reaction rate constant increases with temperature, indicating an accelerated reaction process due to the heightened reaction rate in the intermediate reaction stage with increasing temperature.

According to the Arrhenius equation, the relationship between k and reaction kinetic parameters can be obtained, as shown in Eq. (2)[37]:

$$\ln(\mathrm{k}) = \ln(\mathrm{A}) - \mathrm{Ea}/\mathrm{R}T \quad (2)$$

where, A denotes the pre-factor, R is the gas constant, Ea denotes the activation energy, and T denotes the thermodynamic temperature.

The values of Ea are obtained by fitting Eq. (2). The Arrhenius fit for PE pyrolysis is shown in Fig. 6. Ea for 0, 0.003, and 0.03 V/Å pyrolysis processes are 298.22, 297.47, and 279.27 kJ/mol, respectively. This suggests that the applied electric field reduces Ea during PE pyrolysis. This may be due to the fact that the applied electric field increased the reactive groups within the pyrolysis system.

In order to further investigate the effect of electric field on the pyrolysis process, the variation of the amount of pyrolysis products under three electric field conditions, namely 0, 0.003, and 0.03 V/Å, is studied at a constant temperature (3,300 K), and the results are shown in Fig. 7. As illustrated in Fig. 7a–c, no significant change in the number of C_2H_4, C_2H_2 and H_2 occurs under the influence of the electric field. This indicates that the effect of the electric field on the three final products is not obvious. As shown in Fig. 7d, the amount of CH_4 under electric field conditions increases significantly after 800 ps. The amount of CH_4 at 0.003 V/Å increases rapidly from 800 to 1,500 ps and then stabilizes, while the amount of CH_4 at 0.03 V/Å always shows an increasing trend. However, due to the small amount of CH_4 produced, it is more prone to chance inaccuracy. To investigate changes in the amount of CH_4, changes in the amount of its intermediate products are analyzed. The variation in the number of its major intermediates, CH_3, CH_2, C_2H_4, and C_2H_3, has been studied, and it has been found that conversion of other intermediates (C_4H_9, C_3H_6, C_3H_5, C_3H_4, CH_5, etc.) to CH_4 occurs in the presence of an electric field. The number of decompositions of CH_4 into CH_2 increases from 17 to 22. There are some differences between the different electric fields, with no significant change in the amount of CH_3 present at 0.003 V/Å, but the conversion of CH_3 to CH_4 increases from 21 to 28. At 0.03 V/Å, the amount of CH_3 increases from 31 to 40, resulting in an increase in the amount of CH_4 produced. When the system reacts up to 800 ps, there are sufficient particles present in the system that can be converted to CH_4, so that there appears to be some increase in the number of CH_4 under the electric field.

To better illustrate the reaction network during pyrolysis, we identified and numbered 20 pivotal reactions involving the major products—including both their formation and consumption. These numbered reactions (R1–R20) are detailed in Supplementary Table S1. To explore the influence mechanism of the electric field on polyethylene pyrolysis, the main reactions involving final products (number of net reactions ≥ 10) are analyzed and plotted as shown in Fig. 8. The number of these reactions is the total number for the entire process of pyrolysis. As illustrated in Fig. 8, the generation of C_2H_4 is predominantly attributed to the decomposition of C_3H_7, C_4H_8, C_6H_{12}, C_8H_{16}, and $C_{10}H_{20}$. Combined with the C_2H_4 change curves in Fig. 3, it can be seen that there are more types of reactions to generate C_2H_4, but the number of occurrences of each reaction is relatively less. It has been shown that R4, R5, R6, R7, and R9 are inhibited under the influence of an electric field, resulting in the reduction of C_2H_4. On the one hand, the electric field increases the dipole moment of the molecule, making the angle to the dipole moment increase. On the other hand, due to the decrease of upstream products (e.g., $C_{10}H_{20}$, C_6H_{12}), which in turn leads to the decrease of downstream products (C_8H_{16}, C_4H_8), the reactions R4–R9 are inhibited.

This inhibition enhances with increasing electric field strength, which in turn leads to a negative correlation between the C_2H_4 peak and the electric field strength. C_2H_3, C_2H_2, C_2H_5, and H_2 are generated through R1, R2, R3 and R4. Most of the C_2H_3 is converted to C_2H_2 through R10. Under 0.003 V/Å, R1, R3, R4, and R10 are inhibited and R2 is promoted. Under 0.03 V/Å, R1, R2, R3, R4, and R10 are suppressed, which indicates that the pyrolysis of C_2H_4 is inhibited by the electric field. Under 0.003 V/Å, the hydrogen capture reactions R11 and R14 are promoted, while they are inhibited at 0.03 V/Å. This shows that the electric field affects the PE pyrolysis process by influencing the hydrogen reaction. The main reaction, R18, is less affected by the electric field. However, R19 and R20 are more affected by electric fields, especially under 0.003 V/Å. This suggests

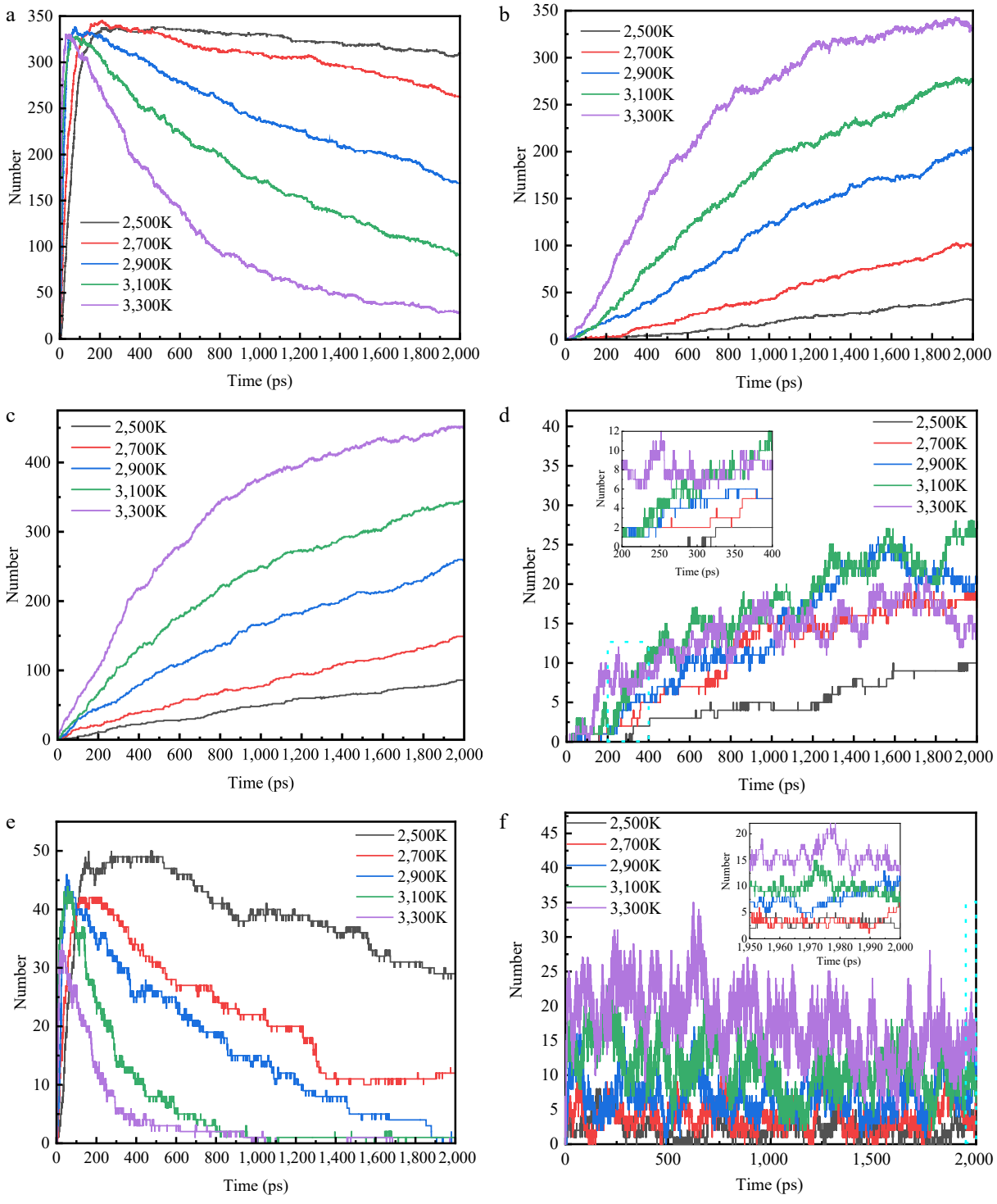

Fig. 5 Plot of changes in the amount of important pyrolysis products at different temperatures. (a) C_2H_4. (b) C_2H_2. (c) H_2. (d) CH_4. (e) C_3H_6. (f) H.

Table 1. Rate constants at different pyrolysis temperatures and electric fields.

Temperature (K)	2,500	2,700	2,900	3,100	3,300
0 V/Å	6.01×10^{10}	2.41×10^{11}	3.39×10^{11}	5.37×10^{11}	3.25×10^{12}
0.003 V/Å	1.41×10^{11}	2.67×10^{11}	4.36×10^{11}	1.24×10^{12}	5.47×10^{12}
0.03 V/Å	4.63×10^{10}	8.04×10^{10}	1.57×10^{11}	3.71×10^{11}	1.36×10^{12}

that the addition of an electric field causes some particles to crack and produce CH_4. In conclusion, the type of polyethylene pyrolysis end product is unaffected by the electric field. However, the key reaction is affected, which affects the PE pyrolysis process. To further investigate the combined effect of temperature and electric field, the electric field and temperature are set to 0.003 V/Å, 2,900 K, and 3,300 K, respectively. The changes in the number of pyrolyzed molecules and chemical reactions are shown by Figs 9 and 10.

As shown in Fig. 9 at 0.003 V/Å, elevated temperatures significantly increase the yields of C_2H_4, C_2H_2, and H_2. This enhancement occurs because the electric field reduces the activation energy barrier for pyrolysis, facilitating chemical bond cleavage and thereby amplifying the temperature sensitivity of the reaction. In order to

analyze the combined effect of electric field and temperature, the percentage of the main reaction products (C_2H_2 and H_2) main reaction is calculated. The percentages of C_2H_2 generated by R10 and R11 are 77.56% and 8.29% (2,900 K), and 72.96% and 11.50% (3,300 K). The percentages of H2 generated by R1, R11, R14, and R15 are 29.23%, 9.05%, 31.32%, and 12.76% (2,900 K), and 35.18%, 6.72%, 19.37%, and 21.74% (3,100 K), respectively. All reaction pathways accelerate under these conditions, though with notable selectivity shifts-some increase proportionally while others decrease. This temperature dependence originates from heightened molecular thermal motion that increases collision frequency and provides activation energy. During PE decomposition, abundant free radicals generated at high temperatures undergo electric field-directed migration. This directional movement alters: (1) molecular collision probabilities, (2) electron density distributions, and (3) radical reaction pathways governing volatile product formation. Furthermore, the field enhances pyrolysis through dual mechanisms: accelerating chain reactions by increasing radical concentration, and reducing activation energies while inducing controlled molecular orientation[32].

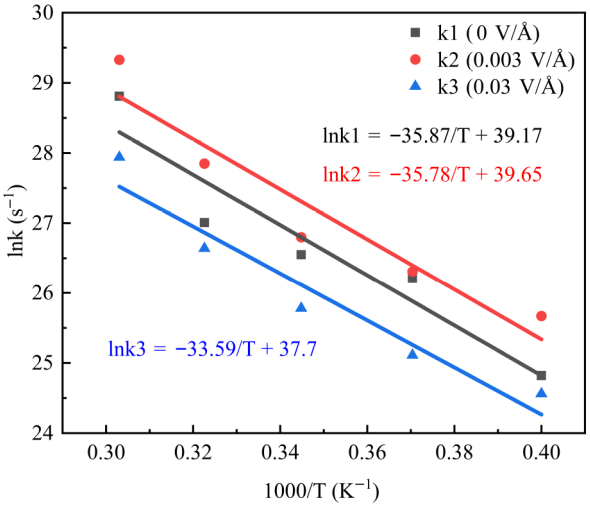

Fig. 6 Kinetic fit of PE pyrolysis rate constant versus temperature.

Mechanisms of influence of electric fields

As illustrated in Fig. 11, the energy changes during pyrolysis vary with the applied electric field. It can be seen that the electric field causes the total energy of the pyrolysis system to decrease, which leads to a decrease in intermolecular potential energy. This suggests that the electric field leads to an increase in the intermolecular distance, which weakens the intermolecular force. The frequency of intermolecular collisions decreases, and partial reactions occur less frequently[32]. In the presence of an electric field, the positive and negative charges in the molecules move away from each other, thus increasing the dipole moment. When the angle between the direction of the electric field and the dipole moment is small, the electric field promotes the reaction, and when the angle between the two is

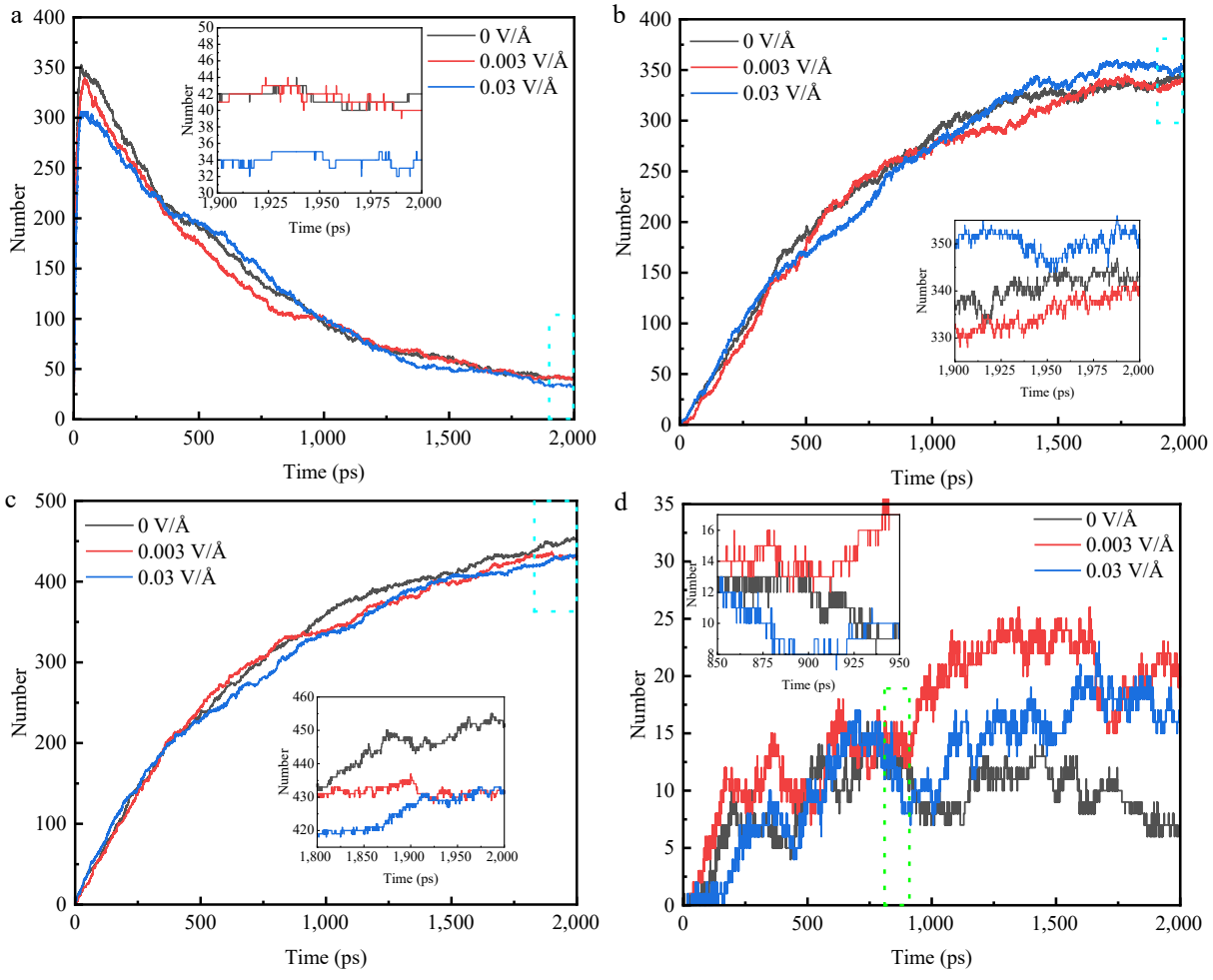

Fig. 7 Variation of the number of major pyrolysis products under different electric fields at 3,300 K. (a) C_2H_4. (b) C_2H_2. (c) H_2. (d) CH_4.

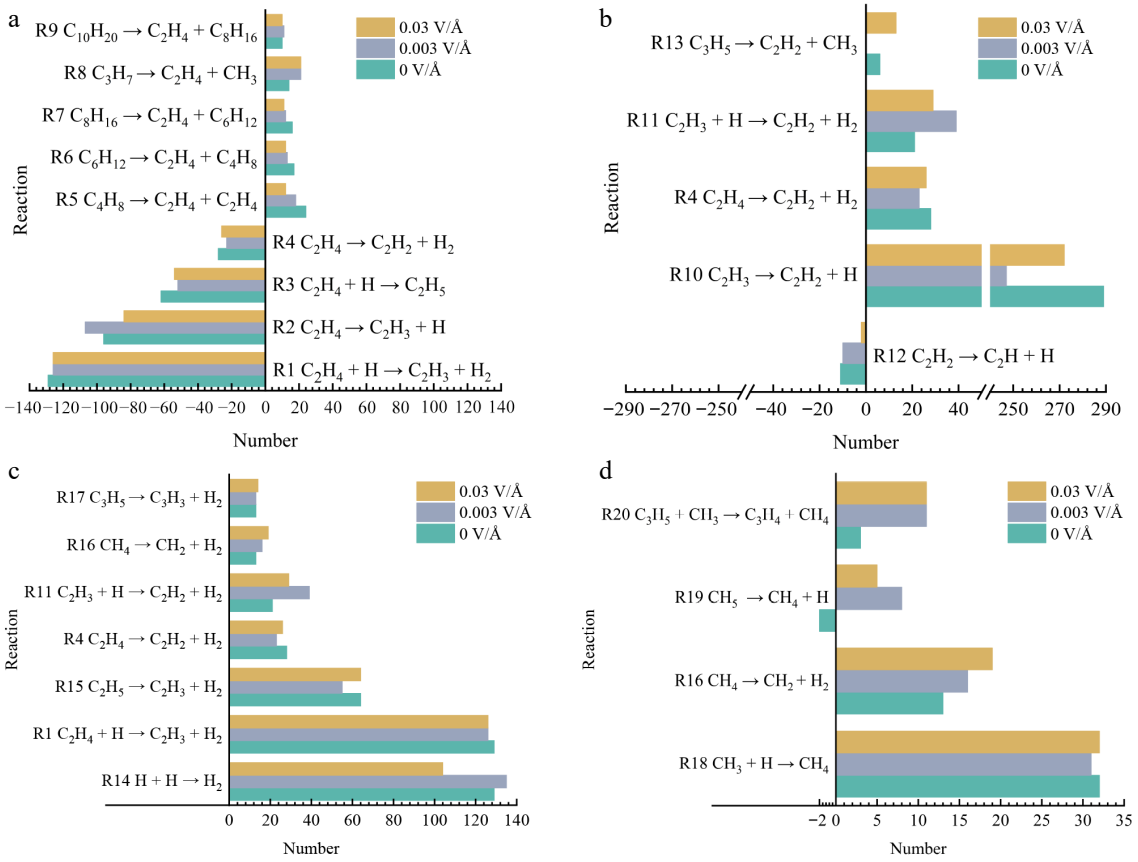

Fig. 8 Major reactions involving major pyrolysis products at different electric fields. (a) C_2H_4. (b) C_2H_2. (c) H_2. (d) CH_4.

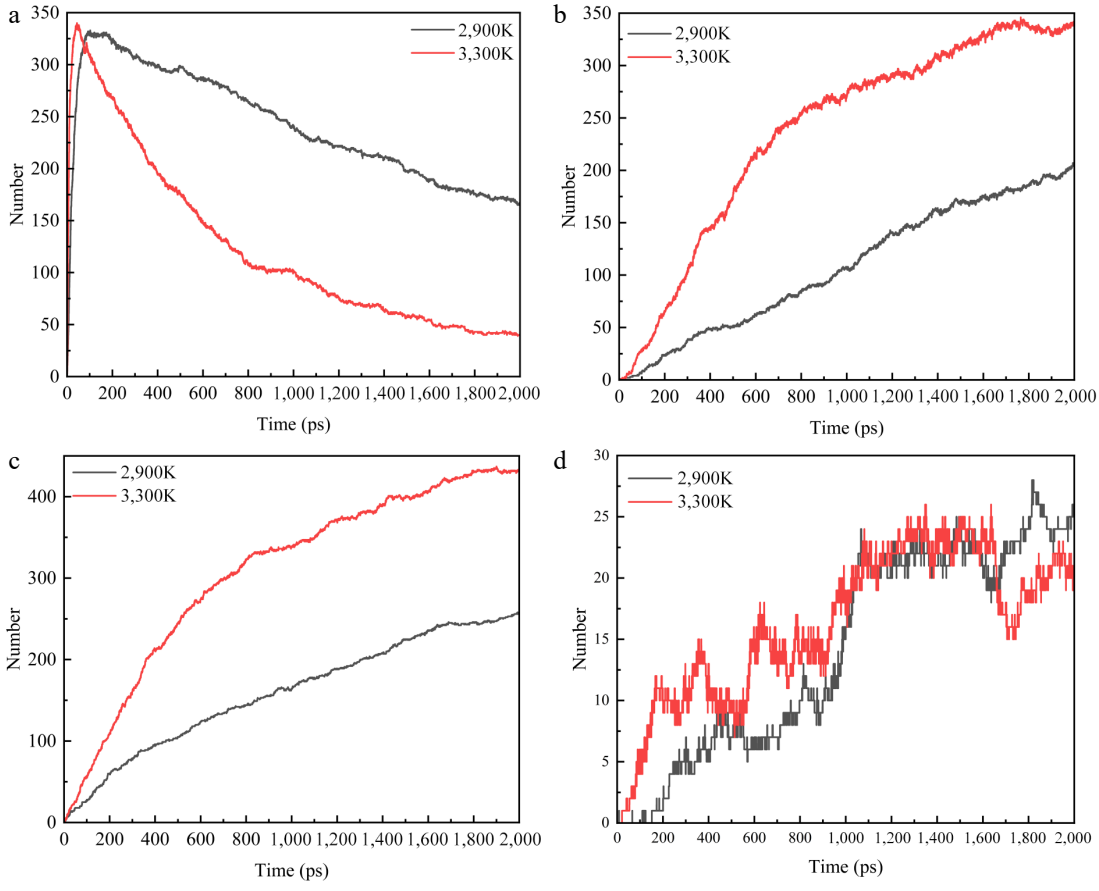

Fig. 9 Plot of changes in the number of pyrolyzed molecules at 2,900 and 3,300 K for specific electric fields. (a) C_2H_4. (b) C_2H_2. (c) H_2. (d) CH_4.

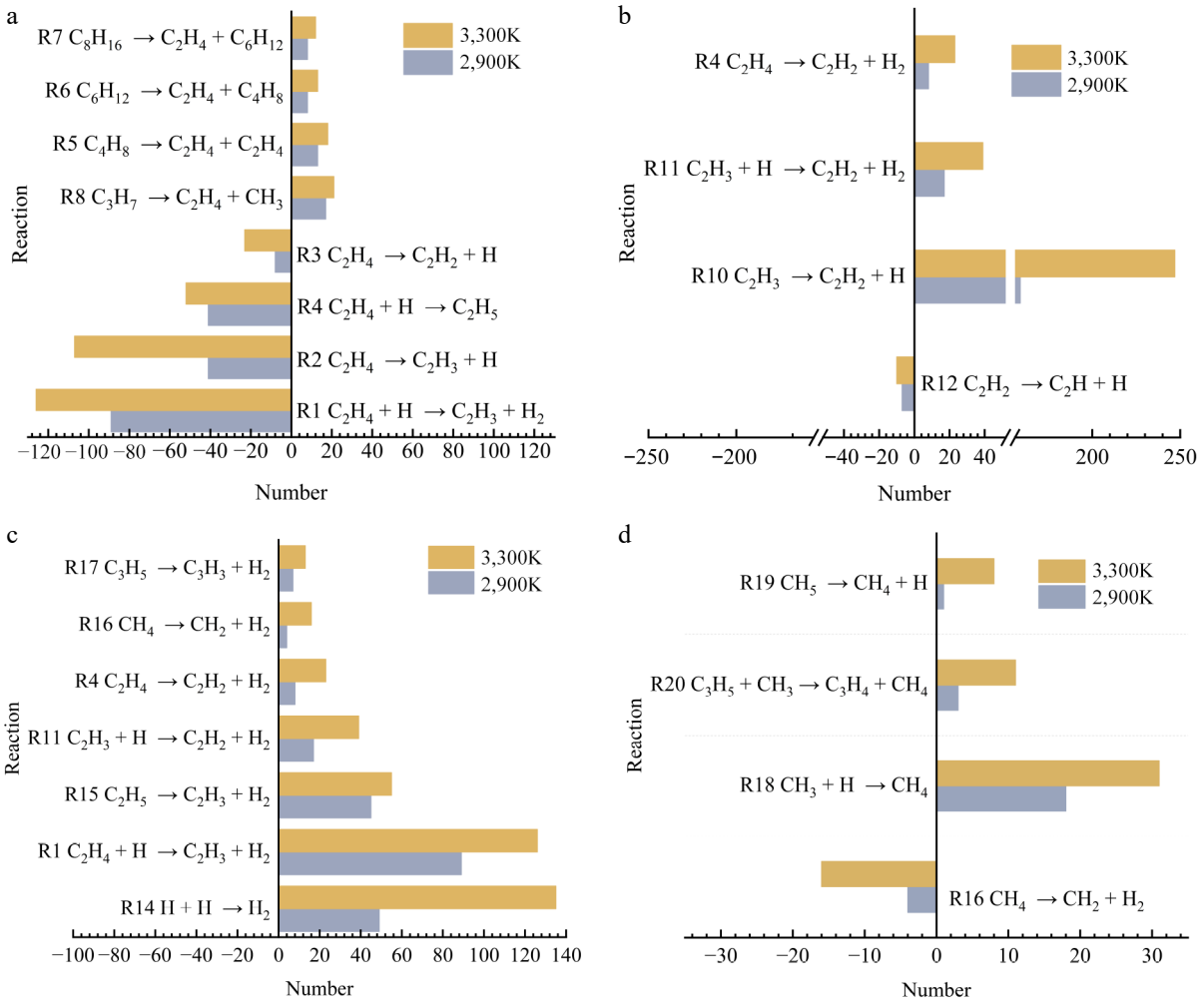

Fig. 10 Plot of the number of major reactions at 2,900 and 3,300 K for specific electric fields. (a) C_2H_4. (b) C_2H_2. (c) H_2. (d) CH_4.

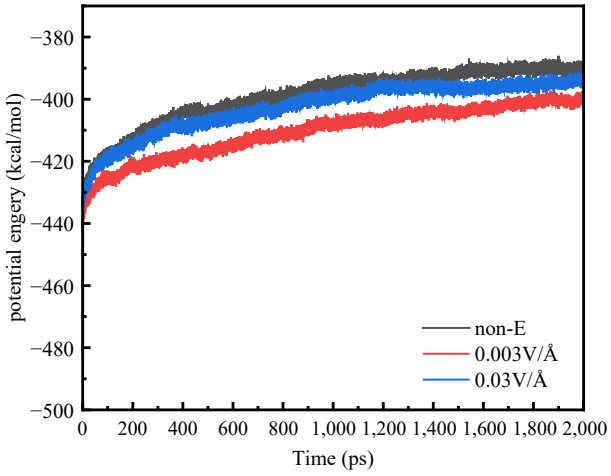

Fig. 11 Potential energy at different electric fields.

large, it produces inhibition[38]. Therefore, different electric fields will have different effects on the same reaction. For example, for R2, the number of reactions occurring increases significantly at 0.003 V/Å, but decreases at 0.03 V/Å instead. This indicates that at 0.003 V/Å, the reaction is promoted by a smaller angle between the electric field direction and the dipole moment, and is inhibited by a larger angle between the electric field direction and the dipole moment at 0.03 V/Å. In addition, the electric field can affect the selectivity of the reaction and the amount of product produced. Using C_2H_2 as an example, at 2,000 ps, the number of C_2H_2 is approximately the same for all three conditions. However, the electric field affected the number of reactions, reducing the share of the core reaction R10 from 84.75% to 72.43% (0.003 V/Å) and 77.49% (0.03 V/Å). At the same time, the share of hydrogen extraction reaction R11 increased from 5.98% to 11.44% (0.003 V/Å) and 8.26% (0.03 V/Å). It is not difficult to find that the effect of the electric field on pyrolysis is multidimensional; firstly, the electric field affects the total energy of the pyrolysis system, and secondly, it can affect the number of times certain reactions take place, which creates selectivity for the reaction and thus affects the pyrolysis process.

Pyrolysis product generation pathway

In order to study the main pathways of PE pyrolysis and the effect of the electric field, Supplementary Table S2 is plotted. As shown in Supplementary Table S2, pyrolysis of PE rarely produces ethylene C_2H_4 directly. Instead, it mainly produces large molecules such as $C_{35}H_{71}$, $C_{65}H_{131}$, $C_{32}H_{65}$, and $C_{68}H_{137}$ through the decomposition process. These larger molecules are further decomposed into smaller particles, and finally, C_2H_4 is generated. This finding suggests that PE pyrolysis is a multi-step decomposition process involving the generation and further decomposition of multiple intermediates. These reaction processes are accidental, and there is no obvious trend. At 0 V/Å, PE is mainly pyrolyzed by C-C single bond fracture.

A simplified schematic of a potential decomposition pathway for PE to C_2H_4 is presented in Supplementary Fig. S1 to illustrate the process. However, under the condition of an electric field, PE will break the C-H bond and generate an H radical. This indicates that the electric field reduces the reaction energy barrier of PE initial pyrolysis or increases the energy of PE initial pyrolysis, which causes the C-H bond to break. C-H breaking increases the number of H radicals in the system. H radicals are the reactive radicals in pyrolysis systems and can make the pyrolysis system more reactive.

At 100 ps, the main species in the system are C_2H_4, C_2H_5, C_2H_3, C_2H_2, CH_4, CH_3, H_2, and H radicals. Some of these species are more active, such as the H radical. It acts as a bridge for reactions throughout the system, reacting with most particles and promoting interparticle transformations. In general, the more H radicals in the system, the more violent the reaction in the system. After 100 ps, the intermediate product C_2H_4 is the dominant reactant. Therefore, the main pyrolysis pathway is plotted using C_2H_4 as the core reactant, as shown in Fig. 12. As shown in Fig. 12, after 100 ps, C_2H_4 is converted to C_2H_3 (71.44%), C_2H_2 (8.88%), and C_2H_5 (19.68%) by dehydrogenation and addition reactions. The conversions under electric field are 75.65%, 7.54% and 16.88% (0.003) and 72.41%, 8.97% and 18.6% (0.03). The vast majority of C_2H_5 is converted to C_2H_3 and H_2 by R15. The main source of decomposition of C_2H_2 is C_2H_3, with a percentage of 91.72% (0 V/Å), 92.56% (0.003 V/Å), and 92.04% (0.03 V/Å) for the three conditions. During the above reaction, H_2 and H radicals are generated, and the percentage of H radicals combining to generate H_2 is 28.48%, 31.11%, and 23.96%. The H radical combines with CH_3 to produce large amounts of CH_4, which is the most important source of CH_4. It is not difficult to find that the electric field affects the selectivity of the reaction, causing a change in the percentage of the reaction involved in the decomposition of C_2H_4 and the formation of C_2H_2, H_2, and CH_4.

Conclusions

In this paper, the pyrolysis process of polyethylene under different temperatures and electric fields is simulated based on ReaxFF-MD. The pyrolysis mechanism of polyethylene and the effect of the electric field on the pyrolysis of polyethylene are analyzed according to the simulation results. The pyrolysis products are then experimentally verified. The following conclusions are drawn:

(1) The final products of PE pyrolysis, as determined by theoretical calculation, consist of C_2H_4, C_2H_2, H_2, and CH_4. This result is consistent with the results of pyrolysis product experiments. The PE pyrolysis system undergoes chain decomposition to produce large amounts of C_2H_4. Subsequently, the majority of the C_2H_4 is involved as the main reactant to produce C_2H_2. Throughout the pyrolysis process, the system generates H radicals and CH_3, which react with products such as C_2H_4 to form H_2 and combine with CH_3 to form CH_4 through dehydrogenation. The key reactions are $C_2H_3 \rightarrow C_2H_2 + H$, $H + C_2H_4 \rightarrow C_2H_3 + H_2$, $H + CH_3 \rightarrow CH_4$ and other reactions.

(2) Under electric field, the number of C_2H_4, C_2H_2, and H_2 do not significantly change, while the number of CH_4 significantly increased. This shows that the electric field has little effect on the types of final products and only changes the quantity of some products. The electric field shows a clear selectivity for the reactions occurring during pyrolysis. The electric field influences the pyrolysis process of PE by regulating the key reaction process. The addition of an electric field increases the distance between molecules and weakens the interaction force between molecules. The frequency of intermolecular collision decreases, and the frequency of partial reactions decreases accordingly, thus changing the reaction path and process of PE pyrolysis.

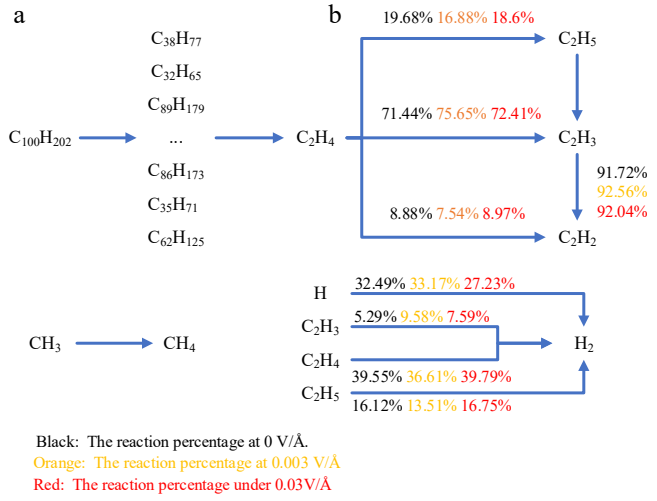

Fig. 12 Generation path of each pyrolysis product after 100 ps. (a) 0.003 V/Å. (b) Strong electric field.

Author contributions

The authors confirm their contributions to the paper as follows: study conception and design: Tian S, Liu B; data collection: Yang D, Liu B; analysis and interpretation of results: Yang D, Wu Y, Maluta NE; draft manuscript preparation: Yang D; supervision and project administration: Huang Z; resource support: Tian S, Li C. All authors reviewed the results and approved the final version of the manuscript.

Data availability

The datasets generated during and analyzed during thecurrent study are available from the corresponding author on reasonable request.

Acknowledgments

This research is supported by the Hubei Provincial Natural Science Foundation project 'Study on the Flame-Retardant Mechanism of Perfluorohexane in High-Voltage Equipment Discharge Fires' (Grant No. 2023AFB956), and the National Natural Science Foundation of China 'Flame Retardant Mechanism and Inhibition of Harmful Products of Perfluorohexane and Mixtures in High-Voltage Equipment Discharge Fires' (Grant No. 52277144).

Conflict of interest

The authors declare that they have no conflict of interest.

Supplementary information accompanies this paper at (https://www.maxapress.com/article/doi/10.48130/prkm-0025-0018)

Dates

Received 3 February 2025; Revised 10 July 2025; Accepted 27 August 2025; Published online 27 October 2025

References

1. Wang W, Huo Y, Kang F, Liu H, Ren H, et al. 2025. Study on hazard of smoke generated by mining cable fires. *Journal of Thermal Analysis and Calorimetry* 150:12175–85

2. Zhang D, Sun YE, Li P, Zhang Y. 2016. Facile fabrication of MoS_2-modified SnO_2 hybrid nanocomposite for ultrasensitive humidity sensing. *ACS Applied Materials & Interfaces* 8(22):14142–49
3. Zhang D, Tong J, Xia B. 2014. Humidity-sensing properties of chemically reduced graphene oxide/polymer nanocomposite film sensor based on layer-by-layer nano self-assembly. *Sensors and Actuators B: Chemical* 197:66–72
4. Zhang X, Yu L, Wu X, Hu W. 2015. Experimental sensing and density functional theory study of H_2S and SOF_2 adsorption on Au-modified graphene. *Advanced Science* 2(11):1500101
5. Cui H, Zhang X, Zhang J, Zhang Y. 2019. Nanomaterials-based gas sensors of SF_6 decomposed species for evaluating the operation status of high-voltage insulation devices. *High Voltage,* 4(4):242–58
6. Chen D, Zhang X, Xiong H, Li Y, Tang J, et al. 2019. A first-principles study of the SF_6 decomposed products adsorbed over defective WS_2 monolayer as promising gas sensing device. *IEEE Transactions on Device and Materials Reliability* 19(3):473–83
7. Wang Y, Kang N, Lin J, Lu S, Liew KM. 2023. On the pyrolysis characteristic parameters of four flame-retardant classes of PVC sheathless cable insulation materials. *Journal of Analytical and Applied Pyrolysis* 170:105901
8. Wang Z, Hostikka S, Wang J. 2022. Pyrolysis behavior and kinetic analysis of waste polypropylene-based complex for cable filler. *Case Studies in Thermal Engineering* 37:102261
9. Liu H, Wang C, Zhang J, Zhao W, Fan M. 2020. Pyrolysis kinetics and thermodynamics of typical plastic waste. *Energy & Fuels* 34(2):2385–90
10. Mamleev V, Bourbigot S, Le Bras M, Lefebvre J. 2004. Three model-free methods for calculation of activation energy in TG. *Journal of Thermal Analysis and Calorimetry* 78:1009–27
11. Chen R, Lu S, Zhang Y, Lo S. 2017. Pyrolysis study of waste cable hose with thermogravimetry/Fourier transform infrared/mass spectrometry analysis. *Energy Conversion and Management* 153:83–92
12. Qin L, Han J, Zhao B, Wang Y, Chen W, et al. 2018. Thermal degradation of medical plastic waste by *in-situ* FTIR, TG-MS and TG-GC/MS coupled analyses. *Journal of Analytical and Applied Pyrolysis* 136:132–45
13. Liu J, Guo X. 2017. ReaxFF molecular dynamics simulation of pyrolysis and combustion of pyridine. *Fuel Processing Technology* 161:107–15
14. van Duin ACT, Dasgupta S, Lorant F, Goddard WA. 2001. ReaxFF: a reactive force field for hydrocarbons. *The Journal of Physical Chemistry A* 105(41):9396–409
15. Chen R, Liu Y, Yin C, Wang L, Zhang L, et al. 2023. A study on the pyrolysis of n-hexane initiated by 1-nitropropane: Molecular dynamics simulations and SVUV-PIMS experiments. *Journal of Analytical and Applied Pyrolysis* 175:106194
16. Cao Y, Liu C, Zhang H, Xu X, Li Q. 2017. Thermal decomposition of HFO-1234yf through ReaxFF molecular dynamics simulation. *Applied Thermal Engineering* 126:330–38
17. Si T, Huang K, Lin Y, Gu M. 2019. ReaxFF study on the effect of CaO on cellulose pyrolysis. *Energy & Fuels* 33(11):11067–77
18. Jung CK, Braunwarth L, Jacob T. 2019. Grand canonical ReaxFF molecular dynamics simulations for catalytic reactions. *Journal of Chemical Theory and Computation* 15(11):5810–16
19. Nie SQ, Chen MQ. 2024. Evaluation on the characteristics of homogeneous catalytic hydrothermal gasification of waste rubber based on ReaxFF-MD simulation. *International Journal of Hydrogen Energy* 51:758–69
20. Ma L, Zhang L, Wang D, Xin H, Ma Q. 2023. Effect of oxygen-supply on the reburning reactivity of pyrolyzed residual from sub-bituminous coal: a reactive force field molecular dynamics simulation. *Energy* 283:129151
21. Liu S, Wei L, Zhou Q, Yang T, Li S, et al. 2023. Simulation strategies for ReaxFF molecular dynamics in coal pyrolysis applications: a review. *Journal of Analytical and Applied Pyrolysis* 170:105882
22. Li YY, Li GY, Zhang H, Wang JP, Li AQ, et al. 2017. ReaxFF study on nitrogen-transfer mechanism in the oxidation process of lignite. *Fuel* 193:331–42
23. Kato T, Yamada Y, Nishikawa Y, Ishikawa H, Sato S. 2021. Carbonization mechanisms of polyimide: Methodology to analyze carbon materials with nitrogen, oxygen, pentagons, and heptagons. *Carbon* 178:58–80
24. Wang Y, Mao Q, Wang Z, Luo KH, Zhou L, et al. 2023. A ReaxFF molecular dynamics study of polycyclic aromatic hydrocarbon oxidation assisted by nitrogen oxides. *Combustion and Flame* 248:112571
25. Pu Y, Liu C, Li Q, Xu X, Huo E. 2020. Pyrolysis mechanism of HFO-1234yf with R32 by ReaxFF MD and DFT method. *International Journal of Refrigeration* 109:82–91
26. Kong J, Zhou K, Ren X, Chen Y, Li Y, et al. 2023. Insight into gaseous product distribution of cross-linked polyethylene pyrolysis using ReaxFF MD simulation and TG-MS. *Journal of Analytical and Applied Pyrolysis* 169:105847
27. Peng C, Chu F, Xu M, Hou J, Zhang W, et al. 2024. Study on the pyrolysis characteristics of styrene-grafted polypropylene cable insulation material. *AIP Advances* 14(2):025134
28. Döntgen M, Przybylski-Freund MD, Kröger LC, Kopp WA, Ismail AE, et al. 2015. Automated discovery of reaction pathways, rate constants, and transition states using reactive molecular dynamics simulations. *Journal of Chemical Theory and Computation* 11(6):2517–24
29. Döntgen M, Schmalz F, Kopp WA, Kroger LC, Leonhard K. 2018. Automated chemical kinetic modeling via hybrid reactive molecular dynamics and quantum chemistry simulations. *Journal of Chemical Information and Modeling* 58(7):1343–55
30. Arvelos S, Abrahão O, Eponina Hori C. 2019. ReaxFF molecular dynamics study on the pyrolysis process of cyclohexanone. *Journal of Analytical and Applied Pyrolysis* 141:104620
31. Zhou W, Zhang X, Zhou W, Yang L, Jia Z. 2022. Inhibition mechanism of electric field on polycyclic aromatic hydrocarbon formation during n-decane pyrolysis: a ReaxFF MD and DFT study. *Journal of the Energy Institute* 102:82–91
32. Zhou W, Zhou W, Yue Y, Jia Z, Yang L. 2023. A ReaxFF and DFT study of effect and mechanism of an electric field on JP-10 fuel pyrolysis. *Journal of the Energy Institute* 111:101445
33. Wood MA, van Duin ACT, Strachan A. 2014. Coupled thermal and electromagnetic induced decomposition in the molecular explosive αHMX; a reactive molecular dynamics study. *The Journal of Physical Chemistry A* 118(5):885–95
34. Hong D, Guo X. 2017. A reactive molecular dynamics study of CH_4 combustion in $O_2/CO_2/H_2O$ environments. *Fuel Processing Technology* 167:416–24
35. Bharti A, Banerjee T. 2016. Reactive force field simulation studies on the combustion behavior of n-octanol. *Fuel Processing Technology* 152:132–39
36. Zhou L, Li F, Wang W, Zhang H, Duan Y, et al. 2025. Effects of phospholipids on pyrolysis and oxidation characteristics of Jatropha biodiesel: TG-FTIR-MS experiment and ReaxFF-MD simulation. *Fuel* 383:133816
37. Liu Q, Liu S, Lv Y, Hu P, Huang Y, et al. 2021. Atomic-scale insight into the pyrolysis of polycarbonate by ReaxFF-based reactive molecular dynamics simulation. *Fuel* 287:119484
38. Yu M, Lou R, Li H, Wang F, Wang J, et al. 2024. Reactive force field molecular dynamics (ReaxFF-MD) simulation of lignite combustion under an external electric field. *Fuel* 358:130184